Cancer Science

WILEY | JCA JAPANESE CANCER ASSOCIATION

ORIGINAL ARTICLE OPEN ACCESS

Single-Cell and Multiomic Analysis Reveals Neutrophil Heterogeneity and Prognostic Value in Cervical Lesions

Ze Wang[1,2] | Liang Zhuang[3] | Shiyi Liu[1,2,4] | Canhui Cao[1,2] | Shimin Chen[5] | Nan Yu[2] | Xiaoyuan Huang[1,2] | Tao Zhang[1,2,6,7]

[1]Department of Gynecologic Oncology, Tongji Hospital, Tongji Medical College, Huazhong University of Science and Technology, Wuhan, Hubei, China | [2]National Clinical Research Center for Obstetrics and Gynecology, Cancer Biology Research Center (Key Laboratory of the Ministry of Education), Tongji Hospital, Tongji Medical College, Huazhong University of Science and Technology, Wuhan, Hubei, China | [3]Department of Oncology, Tongji Hospital, Tongji Medicine College, Huazhong University of Science and Technology, Wuhan, China | [4]Department of Gynecology and Obstetrics, Union Hospital, Tongji Medical College, Huazhong University of Science and Technology, Wuhan, Hubei, China | [5]Wuhan KDWS Biological Technology Co., Ltd, New Technology Platform, Wuhan, China | [6]Reproductive Medicine Center, Department of Obstetrics and Gynecology, Tongji Hospital, Tongji Medicine College, Huazhong University of Science and Technology, Wuhan, China | [7]Shenzhen Huazhong University of Science and Technology Research Institute, Shenzhen, China

Correspondence: Xiaoyuan Huang (huangxy@tjh.tjmu.edu.cn) | Tao Zhang (zhangtao@tjh.tjmu.edu.cn)

Received: 11 July 2025 | **Revised:** 17 November 2025 | **Accepted:** 30 November 2025

Keywords: cervical cancer | cervical lesions | neutrophils | prognostic model | tumor microenvironment

ABSTRACT

Cervical cancer is a prevalent malignancy among women, yet the involvement of neutrophils in its tumor microenvironment remains insufficiently explored. This study utilized single-cell RNA sequencing (scRNA-seq) to delineate neutrophil subsets and elucidate their roles in disease progression and prognosis. Analysis of 20 cervical biopsy samples across different disease stages identified five neutrophil subsets (N0–N4), among which the N4 subset exhibited a marked increase during disease advancement. Spatial transcriptomics and tissue microarray analyses revealed that N4 neutrophils are enriched in tumor regions and are associated with genes implicated in proliferation, metastasis, and immune evasion. Functional characterization demonstrated that N4 promotes tumor progression via activation of the Wnt signaling pathway and extracellular matrix remodeling. A neutrophil infiltration-based risk model was established and validated through multi-omics approaches, highlighting its potential in prognostic prediction. These findings underscore the pivotal role of N4 neutrophils in cervical cancer and provide valuable insights for the development of targeted immunotherapies and personalized treatment strategies.

Abbreviations: BLCA, bladder cancer; BRCA, breast cancer; CC, cervical cancer; CESC, cervical squamous cell carcinoma; CON, control; CSCCs, cervical squamous cell carcinomas; DEGs, differentially expressed genes; DFS, disease-free survival; EGF, epidermal growth factor; GO, gene ontology; HGF, hepatocyte growth factor; HIF-1α, hypoxia-inducible factor 1-α; HSIL, high-grade squamous intraepithelial lesion; HVGs, highly variable genes; IARC, International Agency for Research on Cancer; ICC, invasive cervical squamous cell carcinoma; KNN, K-nearest neighbor; LSIL, low-grade squamous intraepithelial lesions; MIC, microinvasive carcinomas of the cervix; MMPs, matrix metalloproteinases; NES, normalized enrichment score; NETs, neutrophil extracellular traps; NO, nitrogen oxides; NSCLC, non-small lung cell carcinoma; OS, overall survival; PBS, phosphate-buffered saline; PCA, principal component analysis; PDAC, pancreatic ductal adenocarcinoma; PDGF, platelet-derived growth factor; ROC, receiver operating characteristic; ROS, reactive oxygen species; RPE, random priming and extension; ScRNA-seq, single-cell RNA sequencing; TAN, tumor-associated neutrophils; TMA, tissue microarray; TME, the tumor microenvironment; UMAP, unified manifold approximation and projection; uPA, urokinase plasminogen activator; WHO, World Health Organization; WTA, whole transcriptome amplification.

Ze Wang and Liang Zhuang contributed equally to this work.

This is an open access article under the terms of the Creative Commons Attribution-NonCommercial-NoDerivs License, which permits use and distribution in any medium, provided the original work is properly cited, the use is non-commercial and no modifications or adaptations are made.

© 2025 The Author(s). *Cancer Science* published by John Wiley & Sons Australia, Ltd on behalf of Japanese Cancer Association.

1 | Introduction

Cervical cancer (CC) is one of the most common malignant tumors in women worldwide. According to the International Agency for Research on Cancer (IARC) and the World Health Organization (WHO), approximately 600,000 new cases were diagnosed in 2020, accounting for 7.5% of female cancers, making it the fourth most common cancer among women globally. Cervical cancer causes about 340,000 deaths annually, predominantly in developing countries, ranking as the fourth leading cause of cancer-related death in women worldwide [1]. Despite active cervical cancer screening programs and HPV vaccination efforts by WHO and national health agencies, CC remains a major global health challenge, especially in low- and middle-income countries [2]. Therefore, high incidence and mortality rates persist despite prevention advances.

The development of cervical cancer is closely linked to human papillomavirus (HPV) infection, an oncogenic virus associated with nearly all CC cases [3]. Following HPV infection, genomic, transcriptomic, and epigenetic changes accumulate progressively in cervical epithelial cells, leading to cancer through various stages and pathways. The typical progression involves persistent HPV infection, low-grade squamous intraepithelial lesions (LSIL), high-grade squamous intraepithelial lesions (HSIL), and, if untreated, invasive cervical cancer [4]. This multi-stage process offers a valuable window to study early tumor evolution.

The tumor microenvironment (TME) plays a critical role in CC development. It comprises diverse cell types, cytokines, chemokines, extracellular matrix, and vasculature, which collectively regulate tumor proliferation, metastasis, and immune evasion [5]. Among infiltrating immune cells, neutrophils—accounting for ~70% of peripheral white blood cells—are especially abundant. They participate in innate immunity and influence tumor progression via various mechanisms.

Recent studies show neutrophils exert dual roles in tumors. They can promote tumor growth, angiogenesis, and metastasis by secreting cytokines, chemokines, reactive oxygen species, and forming neutrophil extracellular traps (NETs) that facilitate circulating tumor cell capture and metastasis ("pro-tumor effects") [6]. Conversely, under certain conditions, neutrophils exhibit anti-tumor activity, including direct tumor cell killing and inhibition of progression [7]. Thus, neutrophil function in the TME depends on tumor type, immune complexity, and treatment context.

Specifically in cervical cancer, our previous study applied single-cell RNA sequencing (scRNA-seq) to cervical biopsies from 5 healthy controls, 4 HSIL patients, 5 microinvasive carcinoma (MIC) patients, and 6 invasive cervical carcinoma (ICC) patients, analyzing transcriptomes of 120,400 cells [8]. We identified characteristic neutrophil changes during cervical lesion progression and their immune infiltration patterns. Notably, a novel neutrophil subset correlated with cancer progression and poor prognosis. Based on this, we developed a prognostic model emphasizing neutrophils' pivotal role in cervical carcinogenesis and providing a potential biomarker for early diagnosis, treatment selection, and prognosis.

2 | Methods

2.1 | Patient Information and Sample Collection

Twenty cervical biopsies were collected from Tongji Hospital, including 5 healthy controls (HPV^-), 4 high-grade intraepithelial neoplasia (HPV^+), 5 microinvasive cervical carcinoma (HPV^+), and 6 invasive cervical squamous cell carcinoma (HPV^+). Fresh tissues were processed for scRNA-seq. Controls had normal cervices and underwent hysterectomy for uterine fibroids (Table S1) [9].

2.2 | Preparation of Cell Suspension

Tissues were stored in MACS solution, minced (~1 mm^3), and digested with collagenase I and DNase I at 37°C for 45 min. Samples were washed, filtered (70 μm), centrifuged, and treated with erythrocyte lysis buffer. Cells were washed again (PBS with 0.04% BSA), filtered (40 μm), and viability assessed by Calcein-AM and Draq7 staining.

2.3 | ScRNA-Seq Sequencing

Using the BD Rhapsody system, single cells were captured in microwells and paired with barcoded microbeads. After cell lysis, mRNA hybridized to beads, followed by reverse transcription, cDNA amplification, and library construction. Libraries were quantified and sequenced with 150 bp paired-end reads on an Illumina platform.

2.4 | Alignment, Quantification and Quality Control of scRNA-Seq Data

Reads were aligned to GRCh38 using BD software. Cells with fewer than 200 or over 6000 detected genes, or > 50% mitochondrial gene expression, were excluded. Genes expressed in fewer than three cells were removed.

2.5 | Data Normalization and Feature Selection

UMI counts were normalized and log-transformed using Scanpy. The top 2000 highly variable genes were selected for downstream analysis.

2.6 | Dimensionality Reduction and Cluster Analysis

Data were scaled and reduced to 50 principal components by PCA. A neighborhood graph was constructed, and cells were clustered by the Louvain algorithm (resolution 0.5). UMAP was used for visualization.

2.7 | Differential Expression Analysis and Annotation

Cluster marker genes were identified via Wilcoxon rank-sum test (adjusted $p < 0.05$, $\log_2$ fold change > 1).

2.8 | Functional Enrichment Analysis

GSEA was performed with gseapy using hallmark and KEGG gene sets from MSigDB. Differential gene enrichment used clusterProfiler, both with default settings. The "AUCell" function was used to calculate the proportion of cells in each cluster with enrichment of genes in the input KEGG gene set from the area under the curve values. The gene expression of cells was extracted from annotated Harmony objects.

2.9 | Trajectory Analysis

Cell similarity was computed from PCA data to build a KNN graph. The PageRank algorithm identified key cell states along trajectories, visualized on UMAP to reveal progression from normal to cancerous states.

2.10 | Survival Analysis

Kaplan–Meier survival curves and log-rank tests were conducted using the lifelines package.

2.11 | Intercellular Interactions

CellPhoneDB identified ligand-receptor pairs between cell types, with results visualized by Circos plots.

2.12 | Spatial Transcriptome Analysis

Stereo-seq data were processed with Stereopy using a bin size of 100 spots (~$49.72 \times 49.72\,\mu m$) for spatial analysis.

2.13 | Cohort and Immunohistochemistry

Tissue microarrays (85 tumors, 22 adjacent tissues) from Shanghai Outer Biotechnology were stained via the biotin-avidin complex method with antibodies against CK5 (1:400; #71536, Cell signaling), FPR1 (1:400; YT1768, Immunoway), SH3BP5 (1:200; 11127-2-AP, Proteintech). Imaging and quantification were performed using SVI Huygens Suite and HALO platforms.

2.14 | Construction and Validation of the Prognostic Model

LASSO Cox regression established a prognostic model based on neutrophil infiltration. Validation used TCGA-CESC survival data and ROC curve analysis via the pROC package. The risk score and clinicopathological variables were integrated to construct a nomogram.

2.15 | Statistical Analysis

Statistical tests were performed in R using Student's t-test or Wilcoxon test with Bonferroni correction. Significance was defined as two-sided $p < 0.05$. Differential expression required $|\log FC| > 1$ and adjusted $p < 0.05$ ($^*p < 0.05$, $^{**}p < 0.01$, $^{***}p < 0.001$).

3 | Results

3.1 | Correlation Between the Characteristics of Neutrophil Subsets and Cervical Lesions

The study workflow is shown in Figure 1A. We performed single-cell RNA sequencing (scRNA-seq) on 20 cervical biopsy specimens comprising 5 healthy controls (CON), 4 high-grade squamous intraepithelial lesions (HSIL), 5 microinvasive cervical carcinoma (MIC), and 6 invasive cervical squamous cell carcinoma (ICC) samples. Based on canonical marker expression, nine major cell types were identified, including T cells, B cells, squamous and columnar epithelial cells, macrophages, neutrophils, mast cells, fibroblasts, and endothelial cells 9. A total of 2838 neutrophils were isolated for subsequent analysis [8].

Using Uniform Manifold Approximation and Projection (UMAP), we subclustered neutrophils into five discrete subsets (N0 to N4) with distinct transcriptional profiles (Figure 1B–D). Notably, the proportions of N2 and N4 subsets increased progressively with disease severity, from CON to HSIL, MIC, and ICC (Figure 1E), implicating these subpopulations in cervical lesion progression.

Differential gene expression (DEG) analysis revealed subset-specific signatures: N0 cells overexpressed IL4R, suggesting involvement in inflammatory regulation; N1 cells upregulated GLIPR1, possibly linked to proliferation or immune modulation; N2 cells expressed IFITM1, indicative of interferon and antiviral responses; N3 cells showed high CXCR1/2 expression, supporting a role in inflammation; while N4 cells were enriched for genes such as PLAU, CCL4L2, SH3BP5, and LPCAT1, which are implicated in tumor proliferation, metastasis, and immune regulation (Figure 1F,G, Figure S1A,B). PLAU was chosen as a representative marker for the N4 subset to facilitate functional and clinical investigations.

These data delineate neutrophil heterogeneity within cervical lesions and highlight the N4 subset as a potential key driver in the tumor microenvironment (TME) and malignant transformation.

3.2 | Functional Changes and Prognostic Effects of Neutrophil Subsets in the Progression of Cervical Lesions

To investigate functional alterations of neutrophil subsets during cervical lesion progression, we conducted pathway

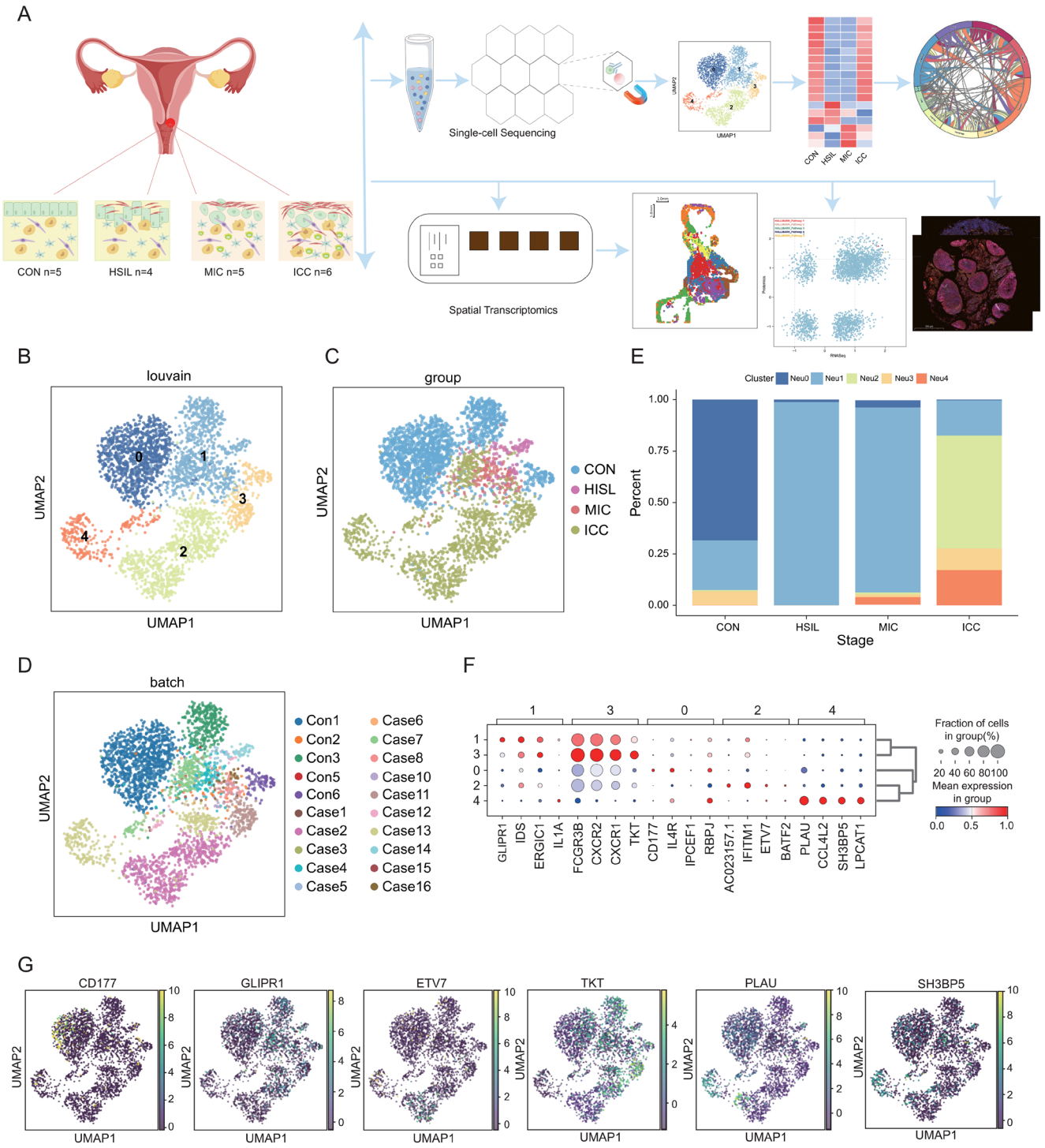

FIGURE 1 | Neutrophil heterogeneity during cervical lesion progression. Single-cell transcriptomic analysis revealed five neutrophil subsets across healthy controls (CON), HSIL, MIC, and ICC stages, with distinct cluster distributions and marker gene expression. (A) Workflow of single-cell neutrophil analysis. (B) UMAP showing five neutrophil clusters ($n = 2838$). (C) UMAP colored by clinical group. (D) UMAP colored by sample ID. (E) Proportional changes in neutrophil subsets across lesion stages. (F) Dot plot of canonical neutrophil markers across clusters. (G) UMAP highlighting representative markers per cluster. Subset annotation was performed using Seurat; comparisons used Wilcoxon tests ($p < 0.05$).

enrichment analyses using GO, KEGG, and Progeny, ssGSEA (Figure 2A, Figure S4A–E). Neutrophils in ICC samples showed pronounced activation of cell cycle-related pathways (G2/M checkpoint, MYC targets, E2F targets) and interferon signaling, potentially reflecting HPV infection–associated oncogenic processes.

Among neutrophil subsets, only N4 showed significant enrichment of immune-related pathways, indicating an immune-active phenotype within the TME (Figure 2C,D, Figure S2A–H). Progeny analysis also associated N4 with hypoxia signaling, suggesting adaptation to the tumor's hypoxic microenvironment (Figure 2B).

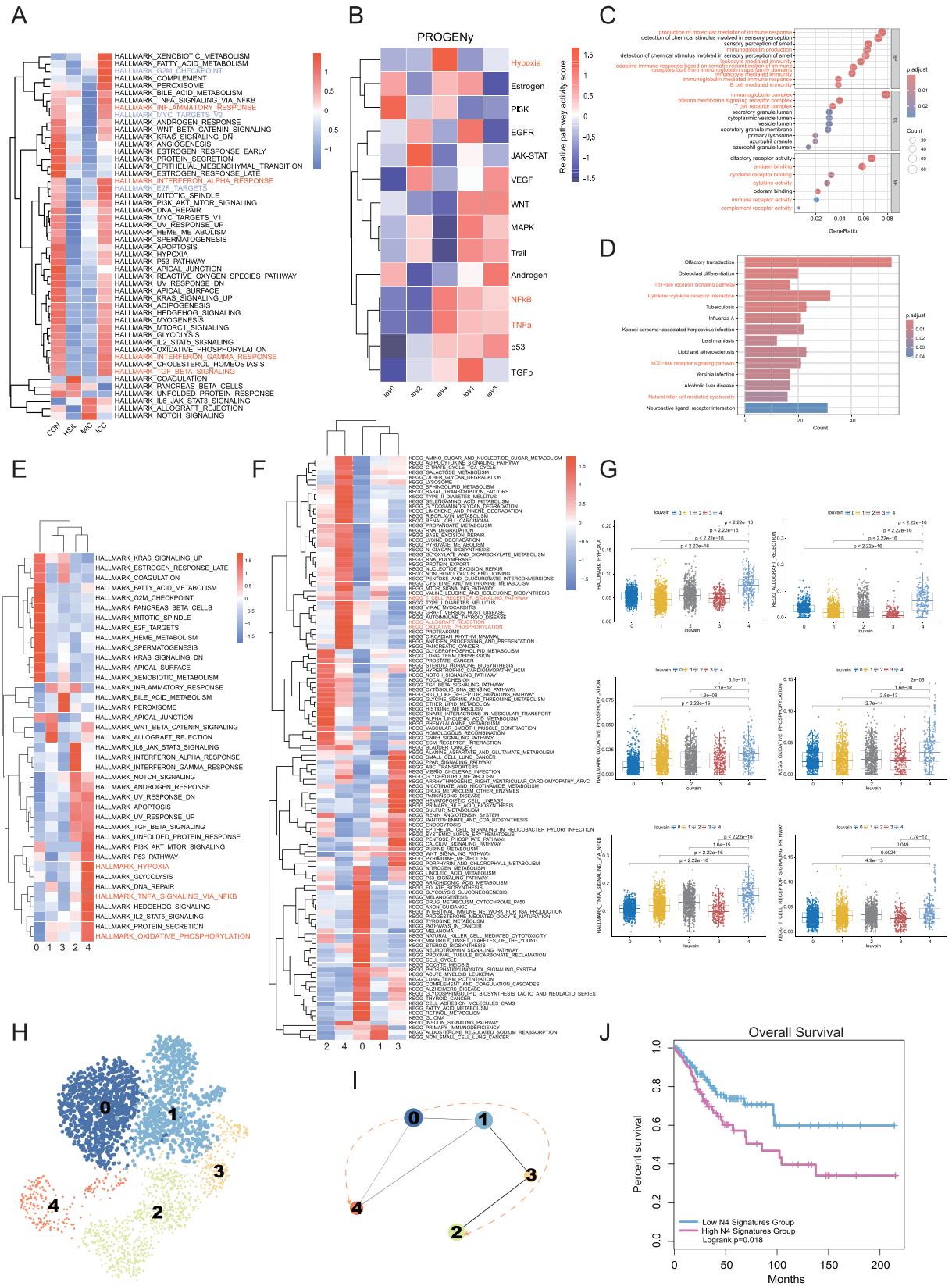

FIGURE 2 | Functional characterization of N4 neutrophils and their prognostic impact. The N4 subset displayed unique pathway enrichment and correlated with poorer prognosis in cervical cancer. (A) Heatmap of ssGSEA pathway scores across subsets. (B) Progeny pathway activity among neutrophil subsets. (C) GO enrichment of N4-specific DEGs. (D) KEGG enrichment of N4-specific DEGs. (E) Heatmap of AUCELL scores for Hallmark pathways in neutrophil clusters. (F) Heatmap of AUCELL scores for KEGG pathways in neutrophil clusters. (G) AUCELL Score Comparison of N0-N4 clusters ($p < 0.05$). (H, I) Pseudotime trajectory showing neutrophil maturation. (J) Kaplan–Meier analysis of TCGA-CESC patients stratified by N4 gene set expression. Pathway analyses used clusterProfiler; survival compared by log-rank test ($n = 304$, TCGA).

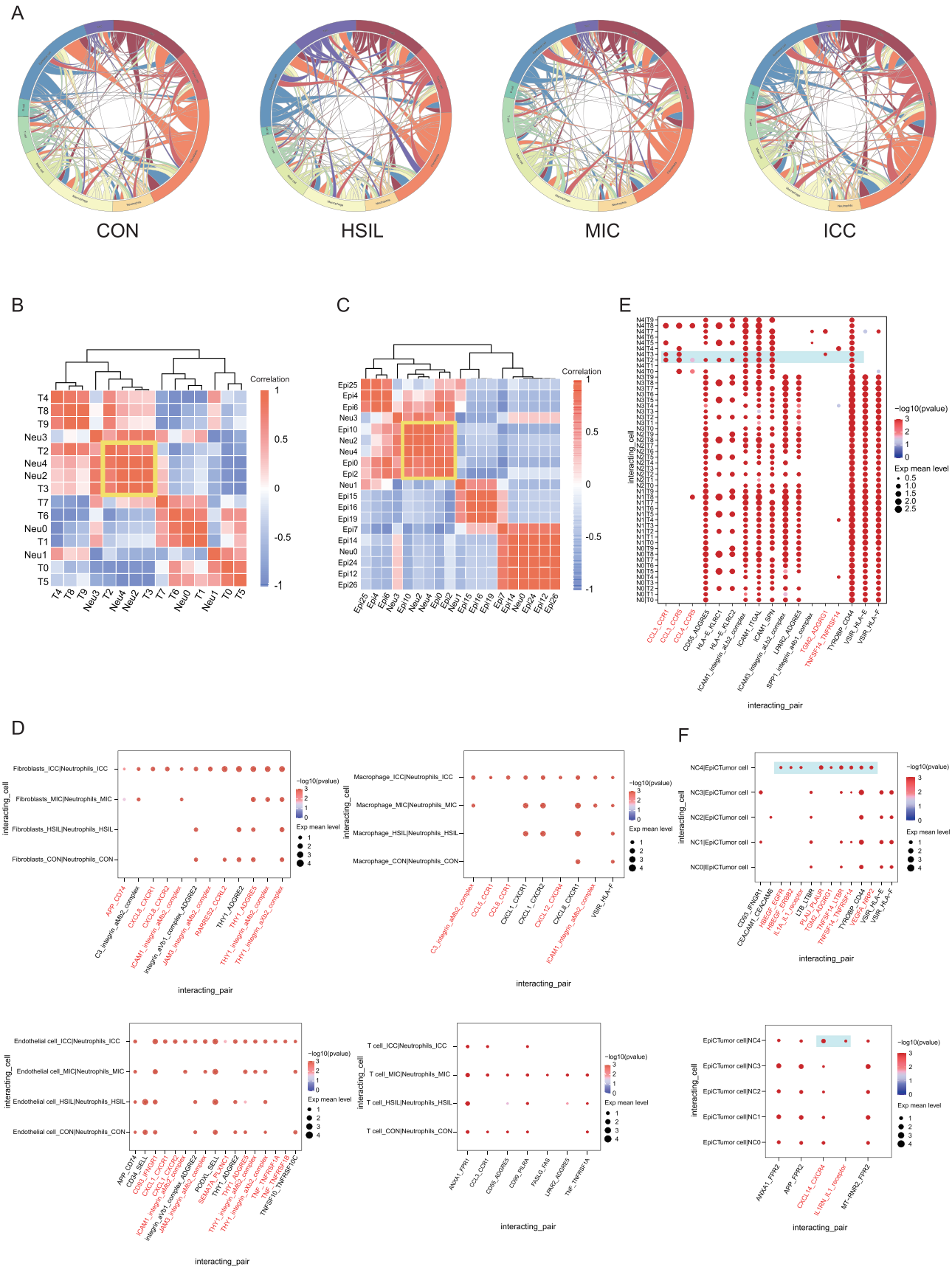

FIGURE 3 | Legend on next page.

FIGURE 3 | Intercellular communication between neutrophils and other cell types. N4 subset showed distinct ligand–receptor interactions with epithelial and immune cells in cervical lesions. (A) Circos plots of ligand–receptor interactions in CON, HSIL, MIC, and ICC. (B) Heatmap showing correlations between neutrophils and T cell subsets. (C) Heatmap of correlations between neutrophils and epithelial subsets. (D) Dot plot of interactions with fibroblasts, macrophages, ECs, and T cells. (E) Neutrophil–T cell ligand–receptor interaction profiles. (F) Neutrophil–epithelial interaction profiles. Interactions were inferred using CellPhoneDB with $p.\text{adjust} < 0.05$.

Transcription factor inference revealed elevated ETS2 [9] and BHLHE40 [10] (inflammatory activation), SOX6 [11] (hypoxia adaptation), and WNT-related NKX3-1 [12], indicating coordinated transcriptional reprogramming (Figure S3F). Consistently, AUCell scoring showed N4 had the highest TNFα, T-cell receptor, hypoxia, and oxidative phosphorylation activity (Figure 2E–G).

Pseudotime trajectory analysis via Monocle2 identified two major differentiation branches with N4 and N2 subsets positioned at terminal, mature differentiation states (Figure 2H,I), implicating these as effector neutrophils during tumor progression.

Survival analysis using TCGA cervical cancer data demonstrated that higher N4 gene signature expression was significantly correlated with worse overall survival (Figure 2J), underscoring the prognostic relevance of this subpopulation. Additionally, preliminary stratification by HPV16/18 revealed distinct functional enrichment (Figure S3A–E).

Overall, these analyses suggest high N4 expression may promote tumor progression via inflammatory, hypoxic, and WNT signaling pathways during cervical lesion development.

3.3 | Intercellular Interactions of Neutrophils in the Microenvironment of Cervical Lesions and Their Effects on Tumor Progression

To understand neutrophil crosstalk with other cell types, we analyzed ligand-receptor interactions among neutrophils, endothelial cells, fibroblasts, macrophages, and T cells at different disease stages (Figure 3A). With lesion progression, interaction frequency and strength increased, notably endothelial-neutrophil pairs (e.g., CD93_IFNGR1, CXCL1_CXCR1/2) facilitating neutrophil transendothelial migration; fibroblast-neutrophil interactions (APP_CD74, CXCL8_CXCR1/2) promoting chemotaxis; and macrophage-neutrophil signaling (CCL5/8_CCR1) enhancing inflammation (Figure 3D).

Correlation analyses revealed strong associations between the N4 neutrophil subset and tumor epithelial cells, as well as exhausted/activated T cell subsets T2 and T3 (Figure 3B,C). Functionally, N4 cells interact with tumor cells through HBEGF_EGFR and HBEGF_ERBB2 signaling, which promote tumor proliferation and with T cell subsets via CCL3/4_CCR1/5 chemokine axes, potentially driving T cell dysfunction and immunosuppression (Figure 3E,F).

Mechanistically, activation of EGFR and ERBB2 by N4-derived HB-EGF is known to initiate canonical oncogenic cascades, including the MAPK/ERK and PI3K/AKT pathways, which drive proliferation, survival, and immune evasion in epithelial cancers [13, 14]. HB-EGF has also been reported to enhance EGFR signaling and reinforce mitogenic responses in the tumor microenvironment [15].

Collectively, these findings identify the N4 subset as a key immunoregulatory population promoting tumor growth and immune escape in cervical cancer.

3.4 | Spatial Distribution and Role of N4 Subpopulation in Tumor Cell Function

To spatially characterize N4 neutrophils and their interaction with tumor cells, we integrated scRNA-seq data with spatial transcriptomics from 15 cervical squamous cell carcinoma samples (Stereo-seq) (Figure 4A, Figure S5A) [16]. This enabled spatial mapping of neutrophil subsets, tumor cells, and fibroblasts (Figure 4B, Figure S5B–C).

Comparing tumor regions enriched or deficient in N4 cells, tumor cells in N4-rich areas exhibited upregulated expression of inflammation-related genes (IGF2R, SLC26A3, S100A6), proliferation markers (RPLP1, RPS8, RPLP2), and Wnt pathway components (IGFBP7) (Figure 4C,D).

GO and KEGG analyses implicated viral response, extracellular matrix remodeling, hypoxia, and immune signaling pathways in these regions (Figure 4F,G). Progeny pathway scoring further identified elevated Wnt, TGF-β, and hypoxia signaling—pathways crucial for epithelial-mesenchymal transition (EMT) and metastasis—in tumor cells co-localized with N4 neutrophils (Figure 4E).

These data highlight the spatial and functional role of N4 neutrophils in fostering a pro-tumor microenvironment, thereby contributing to cervical cancer progression.

3.5 | Tissue Microarray-Based Analysis of N4 Subgroup Infiltration and Its Association With Clinical Characteristics and Prognosis in Cervical Cancer

To validate the clinical relevance of the N4 neutrophil subset, we conducted multiplex immunofluorescence staining on a cervical cancer tissue microarray (TMA) cohort comprising 83 tumor samples and 10 paired adjacent normal tissues (Table S2). The N4 subset was identified by co-expression of the neutrophil marker FPR1 and the N4-specific marker SH3BP5 (Figure 5A,B).

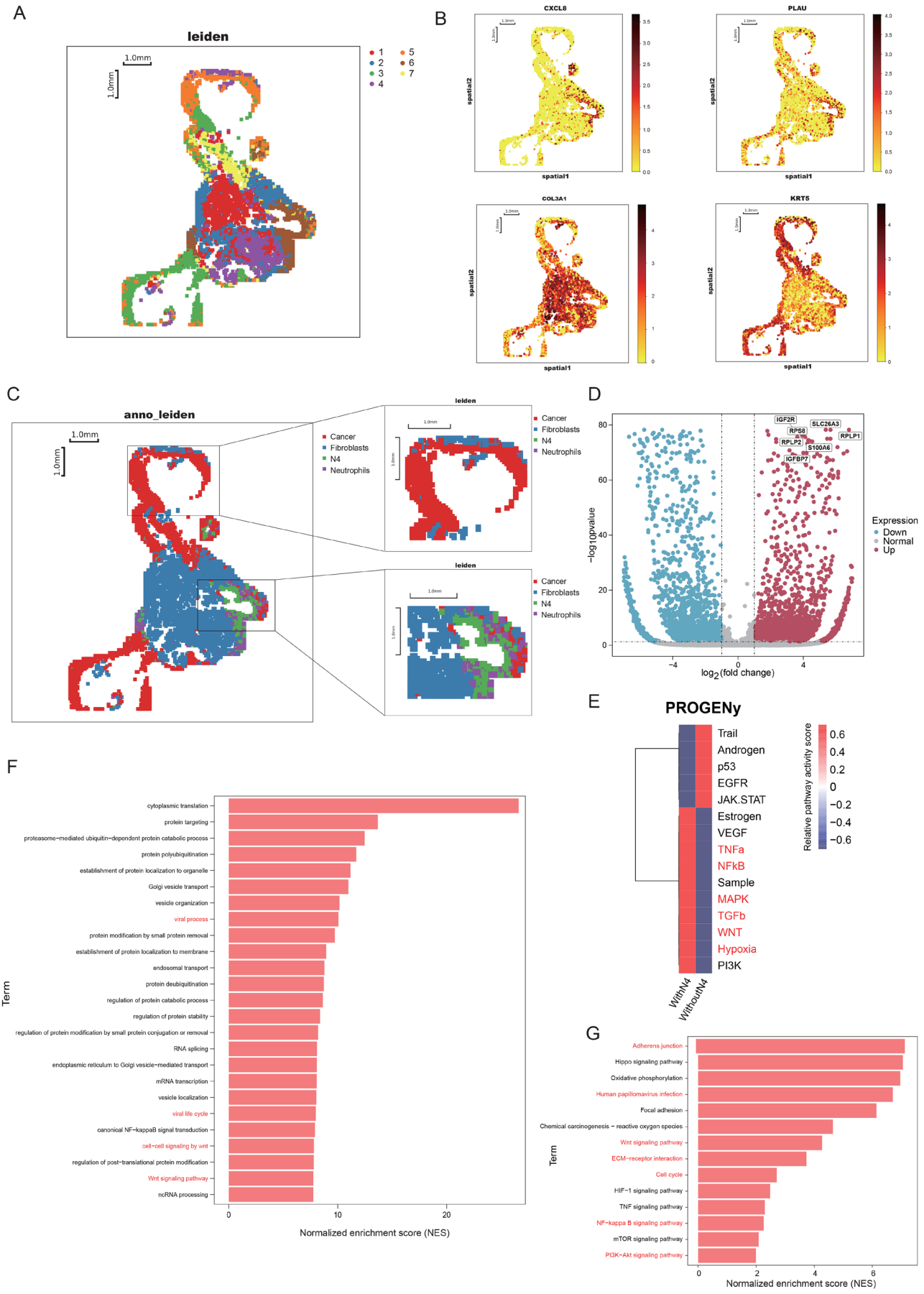

FIGURE 4 | Legend on next page.

FIGURE 4 | Spatial transcriptomics of N4-enriched tumor regions. Integration of single-cell and spatial data identified gene expression patterns in N4-rich tumor niches. (A) Spatial clustering of cell populations. (B) Spatial expression of key marker genes. (C) Definition of N4-enriched and N4-deficient tumor regions. (D) Volcano plot of DEGs between regions. (E) Progeny pathway scores in tumor cells from each region. (F) GO enrichment in N4-enriched region. (G) KEGG enrichment in N4-enriched region. Spatial data analyzed using Seurat and clusterProfiler; DEG cutoff $|\log_2 FC| > 1$, adj.$p < 0.05$.

Survival analyses demonstrated that higher infiltration levels of the N4 subset significantly correlated with poorer overall survival (OS) and disease-free survival (DFS) among cervical cancer patients (Figure 5C,D), corroborating findings from the TCGA cohort. Moreover, patients with tumor recurrence or lymph node metastasis exhibited significantly elevated N4 infiltration compared to their counterparts without these clinical events (Figure 5E,F).

Further stratification by clinical stage revealed that the infiltration ratio of the N4 subset increased progressively from stage I to stage III (Figure 5G), implicating this subpopulation in tumor progression. Additionally, cervical squamous cell carcinoma samples showed higher N4 infiltration compared to other histological subtypes (Figure 5H).

Collectively, these data confirm the presence and clinical impact of the N4 neutrophil subset in cervical cancer, suggesting its potential as a prognostic biomarker and therapeutic target.

3.6 | Evaluation of Prognostic Features Based on Neutrophil Infiltration

To systematically evaluate the prognostic value of neutrophil infiltration, we employed a deconvolution approach to infer neutrophil subset proportions in TCGA cervical cancer bulk RNA-seq data. Utilizing LASSO Cox regression, we developed a risk score model based on neutrophil infiltration levels.

Patients were stratified into high-risk ($n = 126$) and low-risk ($n = 126$) groups according to the median risk score (cutoff = 0.5174). Kaplan–Meier analysis revealed significantly reduced overall survival in the high-risk group (Figure 6A,C, Table S3). Time-dependent ROC curves demonstrated moderate predictive performance for 1-, 2-, and 3-year OS with AUCs ranging from 0.63 to 0.67 (Figure 6D–F), supported by high precision-recall (PR) curve AP values (Figure S5E).

To enhance clinical applicability, we further constructed a prognostic nomogram integrating the risk score with age (≥60 vs. <60 years). The nomogram allowed individualized prediction of 1-, 3-, and 5-year overall survival by mapping total points derived from each variable (Figure 6B). Calibration analysis demonstrated favorable agreement between predicted and observed outcomes, supporting the robustness of the model in clinical risk stratification.

Consistent with prior findings, the high-risk group showed increased infiltration of the N4 subset (Figure 6H). Immune cell infiltration analysis using CIBERSORT revealed enhanced infiltration of plasma cells and mast cells in the low-risk group (Figure 6G), potentially reflecting stronger antiviral immune responses.

Functional enrichment of DEGs between risk groups highlighted upregulation of cell cycle (G2M checkpoint, E2F targets), interferon response (IFN-α/γ), and inflammatory pathways (IL-6/JAK/STAT3 signaling) in the high-risk cohort (Figure 6I). Progeny pathway analysis further identified activation of MAPK, NF-κB, and hypoxia pathways linked to tumor aggressiveness in the high-risk group (Figure 6J, Figure S5F).

These results indicate that neutrophil infiltration patterns, especially N4 dominance, are associated with adverse prognosis and distinct tumor-immune microenvironment characteristics in cervical cancer.

3.7 | Analysis of Immune Activity and Invasion Characteristics of the Tumor Microenvironment in High-Risk Group Cervical Cancer: A Study Based on Multi-Omics Data

To further dissect molecular differences underlying risk stratification, we integrated our single-cell data with bulk transcriptome and proteome datasets ($n = 96$) (Table S4) [17]. Gene set variation analysis (GSVA) revealed enrichment of immune and inflammatory hallmark pathways—including interferon response, IL-6/JAK/STAT3 signaling, and allograft rejection—in the high-risk group at both RNA and protein levels (Figure 7A, Figure S5G).

GO analysis of transcriptomic data emphasized chemokine receptor binding and lymphocyte chemotaxis pathways (Figure 7B), reflecting enhanced immune cell recruitment to the tumor microenvironment. Proteomic data similarly showed enrichment of innate immune activation pathways (Figure 7C).

Notably, GSEA identified chemokine-related pathways as top enriched in the high-risk group, supporting increased cell migration and tumor dissemination potential (Figure 7D). Progeny pathway activity further confirmed upregulation of MAPK, NF-κB, and hypoxia signaling, consistent with aggressive tumor biology (Figure 7E,F).

Differential expression analyses highlighted immune response genes, extracellular matrix remodeling factors, and invasion-associated molecules as significantly upregulated in the high-risk group at RNA (e.g., IGKV1D-13, CCL18, MMP1, RHOXF2, PVRIG2P) and protein levels (e.g., TIPRL, CDK6, ANXA8) (Figure 7G–I). These findings underscore enhanced immune activity, tumor invasiveness, and proliferation as hallmarks of the high-risk cervical cancer microenvironment.

Together, multi-omics evidence reinforces the critical role of neutrophil-mediated immune modulation in cervical

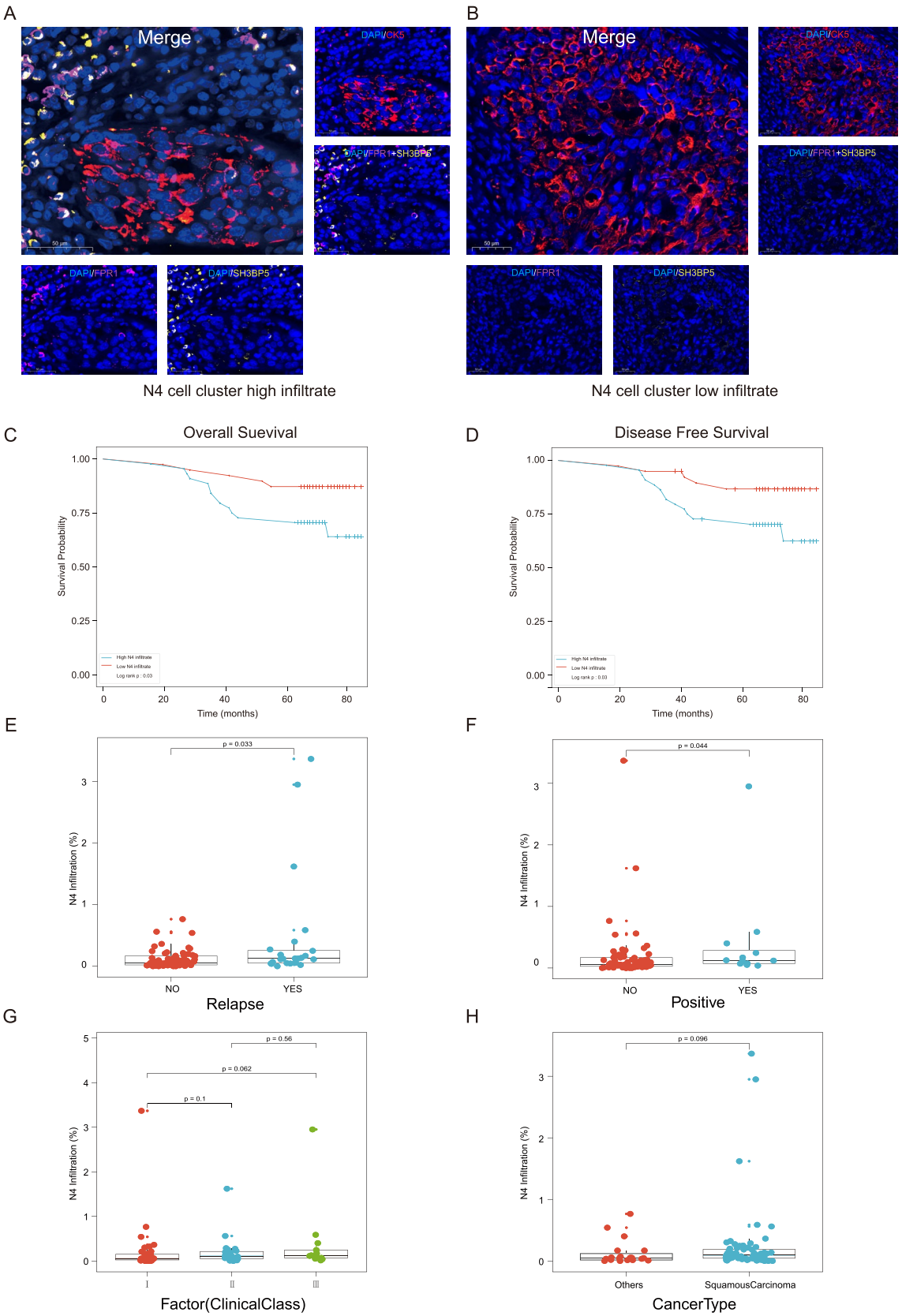

FIGURE 5 | Clinical significance of N4 infiltration in cervical cancer. N4 infiltration levels are associated with survival outcomes and aggressive clinical features. (A, B) Multiplex IF showing FPR1 + SH3BP5+ neutrophils (yellow) in tumor tissues. (C) Kaplan–Meier curve for overall survival (OS, $n = 83$). (D) Kaplan–Meier curve for disease-free survival (DFS). (E) N4 infiltration in recurrence versus non-recurrence groups. (F) Comparison by lymph node metastasis status. (G) Comparison by clinical stage (I–III). (H) Comparison by histological subtype. Statistical analysis: Log-rank test (C, D); Wilcoxon rank-sum test (E–H); $p < 0.05$.

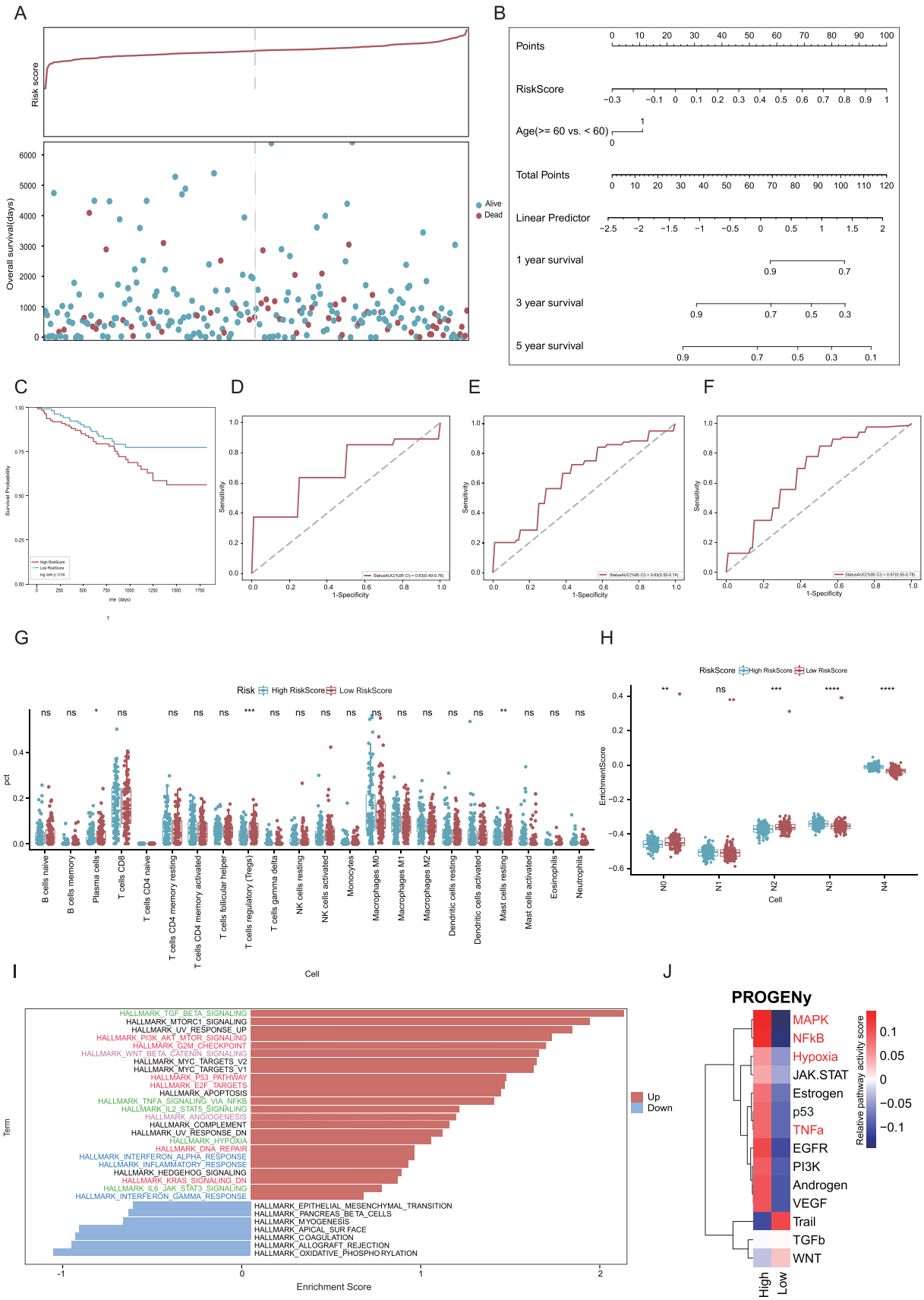

FIGURE 6 | Legend on next page.

FIGURE 6 | Prognostic model based on neutrophil infiltration in TCGA-CESC. A risk score model based on neutrophil features stratifies patients for survival prediction. (A) Distribution of risk scores and survival status. (B) Risk model and clinical information column chart. (C) Kaplan–Meier survival by risk group. (D–F) ROC curves for 1-, 2-, and 3-year mortality prediction. (G) Immune cell infiltration between high- and low-risk groups (CIBERSORT). (H) Distribution of N0–N4 subsets by risk group. (I) GSVA analysis of DEGs. (J) Progeny pathway activity scores. Model constructed using LASSO Cox regression; *p*.adjust < 0.05 considered significant.

cancer progression and provides molecular targets for therapeutic intervention.

4 | Discussion

Neutrophils are the most abundant circulating leukocytes in human blood, playing a critical role in defending against microbial infections and rapidly responding to tissue damage. Despite their prominence, the functional diversity of neutrophils has been less explored compared to other myeloid cells. Recent advances in technologies such as in vivo imaging, high-dimensional transcriptomics, and epigenomics have revealed significant heterogeneity of neutrophils in healthy tissues [18, 19].

Neutrophils contribute to collateral tissue damage during inflammation, yet they also play vital roles in tissue regeneration [20, 21]. This duality is evident in tumor-associated neutrophils (TANs), which can exhibit pro-tumor or anti-tumor functions [22]. Classically, N1 neutrophils mediate anti-tumor effects via cytotoxic molecules such as reactive oxygen species (ROS) and nitrogen oxides (NO) [23], and recruit effector immune cells through cytokines including TNF-α and IL-12, enhancing anti-tumor immunity [24, 25]. However, within the evolving tumor microenvironment (TME), N1 neutrophils can convert to the pro-tumor N2 phenotype, losing their anti-tumor function [26].

Conversely, N2 neutrophils promote tumor progression by secreting vascular endothelial growth factor (VEGF) to stimulate angiogenesis, providing nutrients and oxygen to tumor cells [27]. They also facilitate tumor invasion and metastasis through matrix metalloproteinases (MMPs) secretion [6]and suppress anti-tumor immune responses by releasing immunosuppressive factors like IL-10, impairing T cell and dendritic cell function [28]. These mechanisms underline the critical role of N2 neutrophils at various tumor progression stages [29].

In this study, we applied single-cell RNA sequencing to analyze neutrophils in cervical cancer tissues, aiming to elucidate their role in disease progression. We examined 20 biopsy samples spanning healthy controls (CON), high-grade cervical intraepithelial neoplasia (HSIL), microinvasive cervical cancer (MIC), and invasive cervical squamous cell carcinoma (ICC). Single-cell transcriptomics identified nine major cell types, with a focus on neutrophil subpopulations revealing their significant involvement in the immune response and tumor microenvironment of cervical cancer.

A novel neutrophil subset, N4, was identified, characterized by high expression of PLAU, CCL4L2, SH3BP5, and LPCAT1. PLAU encodes urokinase plasminogen activator (uPA), which catalyzes plasminogen to plasmin, facilitating tumor cell migration, proliferation, and drug resistance [30]. Overexpression of PLAU correlates with poor prognosis in multiple cancers including bladder, head and neck, lung, breast, and cervical cancers [31–37]. Notably, PLAU also relates to neutrophil infiltration, especially in bladder cancer, providing insights into neutrophil subsets in cervical cancer [31].

Our findings showed N4's specific PLAU upregulation in cervical lesions, potentially linking this subpopulation to tumor infiltration and progression. Functionally, N4 was enriched in immune response pathways such as immune receptor activity, immunoglobulin production, and molecular mediator synthesis, indicating a highly inflammatory state. This may enhance N4's infiltration into the tumor microenvironment and promote tumor proliferation through interaction with tumor cells.

Neutrophils are known to secrete growth factors like EGF, HGF, and PDGF related to tumor progression [38, 39]. In our study, N4 interacted with tumor cells via HBEGF_EGFR and HBEGF_ERBB2 signaling, promoting tumor cell proliferation. Importantly, engagement of EGFR and ERBB2 by N4-derived HBEGF is likely to trigger canonical oncogenic cascades, including MAPK/ERK and PI3K/AKT signaling, which are well-established drivers of tumor proliferation, survival, and resistance in epithelial malignancies [14, 25]. This suggests that N4–tumor cell interactions reinforce proliferative signaling beyond ligand–receptor binding, directly integrating into key cancer-associated pathways. The interaction between HBEGF and EGFR/ERBB2 has been implicated in tumor proliferation and metastasis across cancers, including pancreatic ductal adenocarcinoma [40]. Thus, N4 may drive tumor malignancy through these pathways.

Spatial transcriptomics revealed that N4 cells predominantly localized near tumor cells. Within these infiltration zones, tumor cells exhibited upregulated WNT, hypoxia, and viral infection signaling. The WNT pathway, closely linked to HPV infection, is crucial in cervical cancer development, driving tumor proliferation and metastasis [41–43]. Additionally, TMA analysis demonstrated that higher N4 infiltration correlated with adverse clinical outcomes, such as recurrence, lymph node metastasis, and advanced tumor stage. This suggests that N4 may exacerbate tumor malignancy via WNT pathway activation.

Tumor cells in N4 infiltration areas also showed elevated hypoxia-inducible factor 1-α (HIF-1α) signaling. Hypoxia favors neutrophils due to their glycolytic metabolism [44]. HIF-1α promotes PD-L1 expression and inhibits cytotoxic T cell activity, while TANs contribute to hypoxic niches by damaging vasculature, thus facilitating tumor metastasis [45]. These data suggest N4 infiltration not only modulates tumor metabolism but also enhances invasiveness and metastasis through HIF pathway regulation.

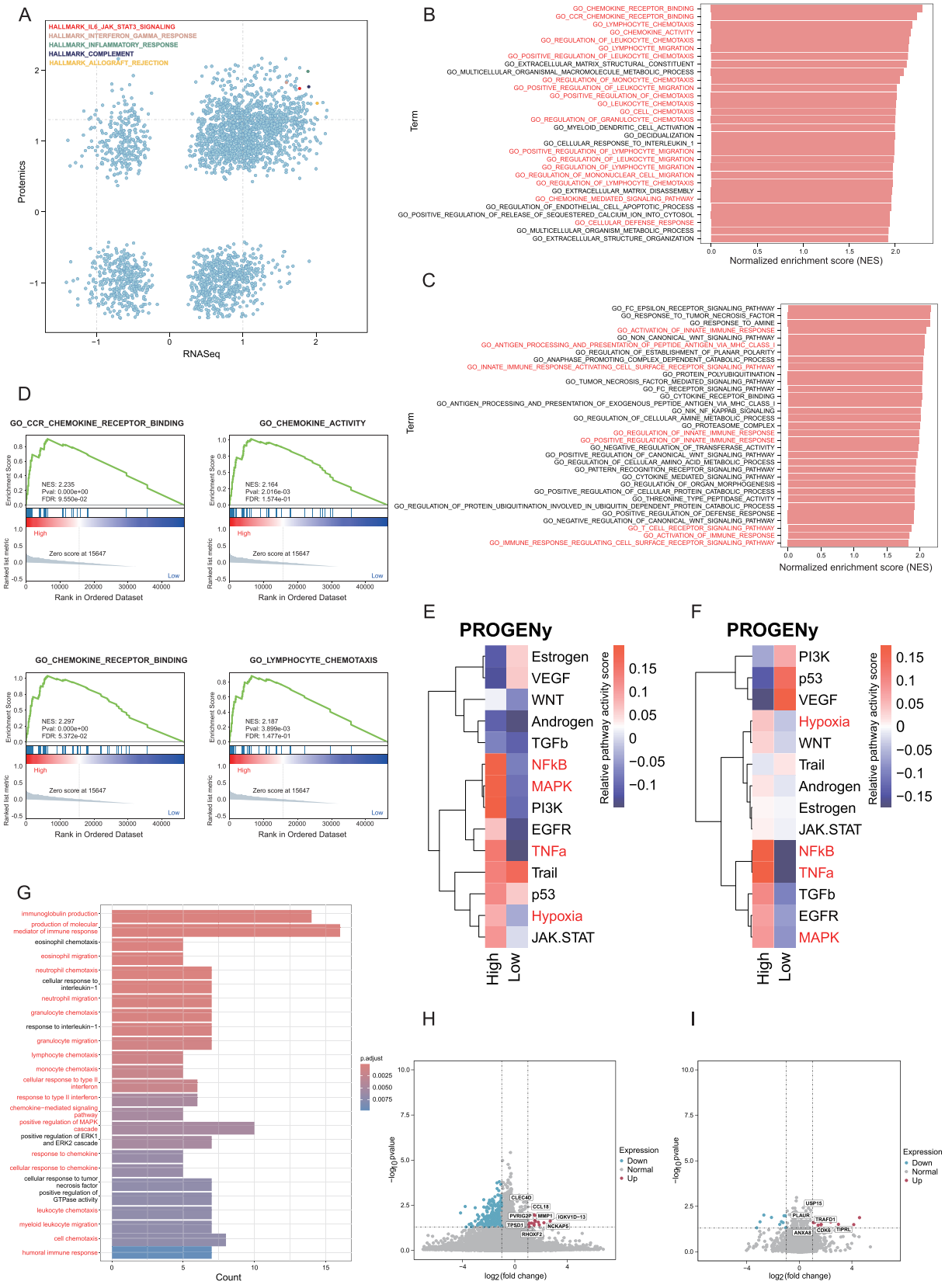

FIGURE 7 | Transcriptomic and proteomic analysis of high- and low-risk groups. High-risk groups exhibited distinct immune and chemokine-related pathway enrichment. (A) NES scatter plot of GSVA terms in transcriptome and proteome. (B, C) GO terms enriched in transcriptome (B) and proteome (C). (D) GSEA results for chemokine-related pathways. (E, F) Progeny scores comparing high- versus low-risk groups. (G) Bar graph of enriched pathways in upregulated DEGs. (H, I) Volcano plots of DEGs in transcriptome (H) and proteome (I). GSVA and GSEA performed with clusterProfiler; DEGs defined with $|\log_2 FC| > 1$, adj.$p < 0.05$.

Single-cell ligand-receptor analysis uncovered dynamic interactions between N4 neutrophils and other cell types—including tumor cells, fibroblasts, endothelial cells, T cells, and macrophages—during disease progression. These interactions likely promote neutrophil migration, activation, and immune suppression. Key mediators included CD93_IFNGR1, CXCL1_CXCR1/2, ICAM1_integrin complexes, APP_CD74, CXCL8_CXCR1/2, THY1_ADGRE5, and CCL5/8_CCR1, CXCL12_CXCR4 pathways, consistent with prior findings highlighting cytokines and chemokines involved in TAN epigenetic regulation and tumor immune microenvironment modulation [46, 47].

Overall, the N4 subpopulation aligns more closely with N2-type neutrophils, yet it uniquely expresses TNF-related pathways, differing from classical N2 profiles. Our pseudotime analysis indicated that N4, like N2, resides at terminal differentiation stages. We conducted an in-depth investigation into the molecular mechanisms underlying the N4 phenotype. Through transcription factor network analysis, we identified ETS2 [9] and BHLHE40 [10] (inflammation-related), SOX6 [11] (hypoxia-related), and NKX3-1 [12] (WNT signaling pathway-related) as potential regulatory factors. Furthermore, pathway scoring based on cell culture experiments revealed that the tumor microenvironment (TME) exhibited the highest levels of TNFα signaling, TCR signaling, hypoxia, and oxidative phosphorylation. Spatial transcriptomics analysis confirmed that N4 regulates TNF and WNT-related signaling pathways in the TME. Collectively, these findings demonstrate that inflammation, hypoxia, and WNT-related signaling collectively drive N4's functional differentiation and tumor-promoting effects. We also speculate that N4 likely maintains tumor inflammation via secretion of IL-8, TNF-α, and modulates the microenvironment through CXCR2, CCL3, and ICAM-1, fostering tumor progression.

Our neutrophil infiltration-based risk scoring model provides a novel prognostic tool for cervical cancer. Evaluating neutrophil subsets enables more precise survival predictions, critical for personalized therapy. The low-risk group exhibited higher immune infiltration, especially plasma cells and mast cells, potentially reflecting immune responses to HPV infection—the main etiological factor in cervical cancer [3, 48]. Differences in immune infiltration likely reflect mechanisms of immune escape and highlight targets for immunotherapy development.

Multi-omics validation (RNA-seq and proteomics) confirmed the high-risk group's tumor microenvironment featured immune activation and inflammation. GO enrichment indicated immune cell chemotaxis and response pathways, supporting immune cell migration and tumor progression. Of note, progeny pathway analysis revealed upregulation of MAPK and NF-kB pathways, and the enrichment of MAPK signaling is consistent with our finding that N4 promotes tumor cell proliferation through EGFR/ERBB2 activation. This convergence highlights MAPK as a central downstream mediator of neutrophil–tumor crosstalk in cervical cancer.

These molecular signatures elucidate the unique tumor microenvironment in high-risk patients, enhancing understanding of cervical cancer progression and providing avenues for novel therapeutic targets, including immune escape, cell migration, and tumor microenvironment interactions.

Limitations include the small sample size (20 samples) and lack of in vitro/in vivo functional validation, which may affect generalizability. Single-cell RNA-seq may underdetect low-abundance cells; future studies should expand sample size and integrate techniques like flow cytometry. Additionally, the prognostic model requires validation in larger clinical cohorts. Future work should explore N4's role in immune escape, develop targeted therapies, and validate clinical applications, offering new strategies for immunotherapy and personalized cervical cancer treatment.

This study applied single-cell RNA sequencing to reveal neutrophil heterogeneity in cervical lesions, emphasizing the immunoregulatory functions of distinct neutrophil subsets, particularly the novel N4 subset. By driving EGFR/ERBB2–MAPK/ERK and PI3K/AKT signaling, N4 promotes tumor progression, metastasis, and immune evasion via interactions with tumor and immune cells and may serve as a biomarker for poor prognosis. These findings provide insight into neutrophil-mediated tumor immunity and suggest targeting neutrophil subpopulations as a potential therapeutic strategy to improve immunotherapy outcomes in cervical cancer.

Author Contributions

Ze Wang: methodology, visualization, writing – original draft. **Liang Zhuang:** writing – review and editing. **Shiyi Liu:** methodology. **Canhui Cao:** methodology, validation. **Shimin Chen:** validation. **Nan Yu:** validation. **Xiaoyuan Huang:** funding acquisition, supervision. **Tao Zhang:** funding acquisition, methodology, supervision, writing – review and editing.

Acknowledgments

The authors have nothing to report.

Funding

This research was supported by the National Natural Science Foundation of China (Grant/Award Number: 82471665), HuBei Provincial Natural Science Foundation of China (Grant/Award Number: 2025AFB047), the Guangdong Provincial Natural Science Foundation of China (Grant/Award Number: 2023A1515010382), Scientific Research Foundation Program of Tongji Hospital (Grant/Award Number: 2024B23), the Education and Research Foundation Program of Second Clinical College of Tongji Medical College of Huazhong University of Science and Technology (Grant/Award Number: TJSZ2024070).

Disclosure

The authors have nothing to report.

Ethics Statement

The study protocol was approved by the Medical Ethics Committee of Tongji Medical College, Huazhong University of Science and Technology. Written informed consent was obtained from all participants. Registry and the Registration No. of S1025.

Consent

All authors agree to publish.

Conflicts of Interest

The authors declare no conflicts of interest.

Data Availability Statement

The authors confirm that the data supporting the findings of this study are available within the articles [8, 16, 17] and their supporting information. Single cell-sequencing is available in the main text, the Supporting Information, and GSA-Human database (https://ngdc.cncb.ac.cn/gsa-human/; ID: sub HRA005765) [8]. The data and scripts supporting the findings of this study have been deposited into CNSA (CNGB Sequence Archive) of CNGBdb (https://db.cngb.org/cnsa/): Stereo-seq data, CNP0002543 [16]. RNA-seq data from this study have been deposited in the National Genomics Data Center (NGDC) under the accession number NGDC: PRJCA009817 [17].

References

1. F. Bray, J. Ferlay, I. Soerjomataram, R. L. Siegel, L. A. Torre, and A. Jemal, "Global Cancer Statistics 2018: GLOBOCAN Estimates of Incidence and Mortality Worldwide for 36 Cancers in 185 Countries," *CA: A Cancer Journal for Clinicians* 68 (2018): 394–424.

2. K. Sundström and K. M. Elfström, "Advances in Cervical Cancer Prevention: Efficacy, Effectiveness, Elimination?," *PLoS Medicine* 17 (2020): e1003035.

3. E. J. Crosbie, M. H. Einstein, S. Franceschi, and H. C. Kitchener, "Human Papillomavirus and Cervical Cancer," *Lancet* 382 (2013): 889–899.

4. W. Cb, C. Si, and Y. Ls, "The Natural History of Cervical HPV Infection: Unresolved Issues," *Nature Reviews. Cancer* 7 (2007): 11–22.

5. P. Ms, F. Mlm, and C. Am, "Purinergic Signaling and Tumor Microenvironment in Cervical Cancer," *Purinergic Signalling* 16 (2020): 123–135.

6. S. B. Coffelt, M. D. Wellenstein, and K. E. de Visser, "Neutrophils in Cancer: Neutral no More," *Nature Reviews. Cancer* 16 (2016): 431–446.

7. P. Bouti, X. W. Zhao, P. J. J. H. Verkuijlen, et al., "Kindlin3-Dependent CD11b/CD18-Integrin Activation Is Required for Potentiation of Neutrophil Cytotoxicity by CD47-SIRPα Checkpoint Disruption," *Cancer Immunology Research* 9 (2021): 147–155.

8. T. Zhang, L. Zhuang, M. Muaibati, et al., "Identification of Cervical Cancer Stem Cells Using Single-Cell Transcriptomes of Normal Cervix, Cervical Premalignant Lesions, and Cervical Cancer," *eBioMedicine* 92 (2023): 104612.

9. F. W. Miller, "The Increasing Prevalence of Autoimmunity and Autoimmune Diseases: An Urgent Call to Action for Improved Understanding, Diagnosis, Treatment, and Prevention," *Current Opinion in Immunology* 80 (2023): 102266.

10. S. Yang, D. Zhang, Q. Sun, et al., "Single-Cell and Spatial Transcriptome Profiling Identifies the Transcription Factor BHLHE40 as a Driver of EMT in Metastatic Colorectal Cancer," *Cancer Research* 84 (2024): 2202–2217.

11. Y. Wang, S. Wang, D. Chen, et al., "Regulation of Hypoxia-Induced Proliferation of Human Pulmonary Artery Smooth Muscle Cells by SOX6-SOCS3 Through the STAT3 Signaling Pathway," *Journal of the Third Military Medical University* 43 (2021): 295–302.

12. M. Kruithof-de Julio, M. Shibata, N. Desai, et al., "Canonical Wnt Signaling Regulates Nkx3.1 Expression and Luminal Epithelial Differentiation During Prostate Organogenesis," *Developmental Dynamics* 242 (2013): 1160–1171.

13. P. Wee and Z. Wang, "Epidermal Growth Factor Receptor Cell Proliferation Signaling Pathways," *Cancers (Basel)* 9 (2017): 52.

14. N. E. Hynes and G. MacDonald, "ErbB Receptors and Signaling Pathways in Cancer," *Current Opinion in Cell Biology* 21 (2009): 177–184.

15. K. Miyata, F. Yotsumoto, S. O. Nam, M. Kuroki, and S. Miyamoto, "Regulatory Mechanisms of the HB-EGF Autocrine Loop in Inflammation, Homeostasis, Development and Cancer," *Anticancer Research* 32 (2012): 2347–2352.

16. Z. Ou, S. Lin, J. Qiu, et al., "Single-Nucleus RNA Sequencing and Spatial Transcriptomics Reveal the Immunological Microenvironment of Cervical Squamous Cell Carcinoma," *Advanced Science* 9 (2022): e2203040.

17. J. Fan, Y. Fu, W. Peng, et al., "Multi-Omics Characterization of Silent and Productive HPV Integration in Cervical Cancer," *Cell Genomics* 3 (2023): 100211.

18. V. Naranbhai, B. P. Fairfax, S. Makino, et al., "Genomic Modulators of Gene Expression in Human Neutrophils," *Nature Communications* 6 (2015): 7545.

19. F. S. Lakschevitz, M. B. Visser, C. Sun, and M. Glogauer, "Neutrophil Transcriptional Profile Changes During Transit From Bone Marrow to Sites of Inflammation," *Cellular & Molecular Immunology* 12 (2015): 53–65.

20. F. X. Pizza, J. M. Peterson, J. H. Baas, and T. J. Koh, "Neutrophils Contribute to Muscle Injury and Impair Its Resolution After Lengthening Contractions in Mice," *Journal of Physiology* 562 (2005): 899–913.

21. H. Toumi, S. F'guyer, and T. M. Best, "The Role of Neutrophils in Injury and Repair Following Muscle Stretch," *Journal of Anatomy* 208 (2006): 459–470.

22. J. Wang, "Neutrophils in Tissue Injury and Repair," *Cell and Tissue Research* 371 (2018): 531–539.

23. M. Herre, J. Cedervall, N. Mackman, and A. K. Olsson, "Neutrophil Extracellular Traps in the Pathology of Cancer and Other Inflammatory Diseases," *Physiological Reviews* 103 (2023): 277–312.

24. S. Jaillon, A. Ponzetta, D. Di Mitri, A. Santoni, R. Bonecchi, and A. Mantovani, "Neutrophil Diversity and Plasticity in Tumour Progression and Therapy," *Nature Reviews. Cancer* 20 (2020): 485–503.

25. C. Silvestre-Roig, Z. G. Fridlender, M. Glogauer, and P. Scapini, "Neutrophil Diversity in Health and Disease," *Trends in Immunology* 40 (2019): 565–583.

26. M. E. Shaul and Z. G. Fridlender, "Tumour-Associated Neutrophils in Patients With Cancer," *Nature Reviews. Clinical Oncology* 16 (2019): 601–620.

27. F. Veglia, E. Sanseviero, and D. I. Gabrilovich, "Myeloid-Derived Suppressor Cells in the Era of Increasing Myeloid Cell Diversity," *Nature Reviews. Immunology* 21 (2021): 485–498.

28. L. Wu, S. Saxena, M. Awaji, and R. K. Singh, "Tumor-Associated Neutrophils in Cancer: Going Pro," *Cancers (Basel)* 11 (2019): 564.

29. L. Yang, Q. Liu, X. Zhang, et al., "DNA of Neutrophil Extracellular Traps Promotes Cancer Metastasis via CCDC25," *Nature* 583 (2020): 133–138.

30. P. F. M. Choong and A. P. W. Nadesapillai, "Urokinase Plasminogen Activator System: A Multifunctional Role in Tumor Progression and Metastasis," *Clinical Orthopaedics and Related Research* 215 (2003): S46–S58.

31. K. Shi, J. Zhou, M. Li, et al., "Pan-Cancer Analysis of PLAU Indicates Its Potential Prognostic Value and Correlation With Neutrophil Infiltration in BLCA," *Biochimica et Biophysica Acta – Molecular Basis of Disease* 1870 (2024): 166965.

32. Z. Li, C. Chen, J. Wang, et al., "Overexpressed PLAU and Its Potential Prognostic Value in Head and Neck Squamous Cell Carcinoma," *PeerJ* 9 (2021): e10746.

33. Z.-C. Guo, S.-L. Jing, H. Cui, L.-Y. Xie, S.-J. Na, and J.-B. Tu, "PLAU and LAMC2 Can Predict a Poor Prognosis in Patients With HNSCC," *Journal of Cancer* 14 (2023): 1660–1672.

34. X. Cui, H. Sun, X. Liu, et al., "PLAU Promotes Cell Proliferation and Migration of Head and Neck Cancer via STAT3 Signaling Pathway," *Experimental Cell Research* 438 (2024): 114056.

35. Y. Zheng, L. Zhang, K. Zhang, et al., "PLAU Promotes Growth and Attenuates Cisplatin Chemosensitivity in ARID1A-Depleted Non-Small Cell Lung Cancer Through Interaction With TM4SF1," *Biology Direct* 19 (2024): 7.

36. Y. Wang, M. Zhu, J. Li, et al., "Overexpression of PSMC2 Promotes the Tumorigenesis and Development of Human Breast Cancer via Regulating Plasminogen Activator Urokinase (PLAU)," *Cell Death & Disease* 12 (2021): 690.

37. Y. Gao, X. Ma, H. Lu, P. Xu, and C. Xu, "PLAU Is Associated With Cell Migration and Invasion and Is Regulated by Transcription Factor YY1 in Cervical Cancer," *Oncology Reports* 49 (2023): 25.

38. Z. Granot and J. Jablonska, "Distinct Functions of Neutrophil in Cancer and Its Regulation," *Mediators of Inflammation* 2015 (2015): 701067.

39. C. Tecchio, P. Scapini, G. Pizzolo, and M. A. Cassatella, "On the Cytokines Produced by Human Neutrophils in Tumors," *Seminars in Cancer Biology* 23 (2013): 159–170.

40. K. Yang, T. Yang, J. Yu, F. Li, and X. Zhao, "Integrated Transcriptional Analysis Reveals Macrophage Heterogeneity and Macrophage-Tumor Cell Interactions in the Progression of Pancreatic Ductal Adenocarcinoma," *BMC Cancer* 23 (2023): 199.

41. T. Zhang, Z. Wang, M. Muaibati, et al., "Natural Small Molecule Compounds Targeting Wnt Signaling Pathway Inhibit HPV Infection," *Microbial Pathogenesis* 196 (2024): 106960.

42. C. Chumduri, R. K. Gurumurthy, H. Berger, et al., "Opposing Wnt Signals Regulate Cervical Squamocolumnar Homeostasis and Emergence of Metaplasia," *Nature Cell Biology* 23 (2021): 184–197.

43. T. Xu, Y. Zeng, L. Shi, et al., "Targeting NEK2 Impairs Oncogenesis and Radioresistance via Inhibiting the Wnt1/β-Catenin Signaling Pathway in Cervical Cancer," *Journal of Experimental & Clinical Cancer Research* 39 (2020): 183.

44. S.-W. Jing, Y.-D. Wang, M. Kuroda, et al., "HIF-1α Contributes to Hypoxia-Induced Invasion and Metastasis of Esophageal Carcinoma via Inhibiting E-Cadherin and Promoting MMP-2 Expression," *Acta Medica Okayama* 66 (2012): 399–407.

45. K. Mahiddine, A. Blaisdell, S. Ma, A. Créquer-Grandhomme, C. A. Lowell, and A. Erlebacher, "Relief of Tumor Hypoxia Unleashes the Tumoricidal Potential of Neutrophils," *Journal of Clinical Investigation* 130 (2020): 389–403.

46. Z. G. Fridlender, J. Sun, I. Mishalian, et al., "Transcriptomic Analysis Comparing Tumor-Associated Neutrophils With Granulocytic Myeloid-Derived Suppressor Cells and Normal Neutrophils," *PLoS One* 7 (2012): e31524.

47. X. Wu, J. Xia, Z. Wang, et al., "Feiyanning Downregulating CXCLs/CXCR2 Axis to Suppress TANs Infiltration in the Prevention of Lung Cancer Metastasis," *Journal of Ethnopharmacology* 295 (2022): 115277.

48. H. Gonzalez, C. Hagerling, and Z. Werb, "Roles of the Immune System in Cancer: From Tumor Initiation to Metastatic Progression," *Genes & Development* 32 (2018): 1267–1284.

Supporting Information

Additional supporting information can be found online in the Supporting Information section. **Figure S1:** Characterization of neutrophil subsets based on canonical marker genes. **Figure S2:** GO and KEGG enrichment analyses of top DEGs in neutrophil subsets. **Figure S3:** Functional enrichment and transcription factor activity analyses across HPV genotypes. **Figure S4:** Functional pathway enrichment and ligand–receptor interaction analyses of neutrophil subsets. **Figure S5:** Integration of single-cell and transcriptome data and functional characterization of risk groups. **Table S1:** Characteristics of the 20 patients included in this study [9]. **Table S2:** Sample Information of Cervical Cancer Tissue Microarray ($n = 83$). **Table S3:** High-and low-risk grouping of the overall patients in the TCGA-CESC database. **Table S4:** High-and low-risk grouping of patients in the multi-omics database.